[3] Whetstone, W. D., "Computer Analysis of Large Linear Frames," *Proceedings of the ASCE, Journal of the Structural Division*, Vol. 95, Nov. 1969, pp. 2401–2417.

[4] Cruse, I. A., "Numerical Solutions in Three-Dimensional Elastostatics," *International Journal of Solids and Structures*, Vol. 5, 1969, pp. 1259–1274.

[5] Deak, A. L., "Numerical Solution of Three-Dimensional Elasticity Problems for Solid Rocket Grains Based on Integral Equations," AFRPL-TR-71-140, Feb. 1972, Air Force Rocket Propulsion Lab., Wright-Patterson Air Force Base, Ohio.

# Scattering Properties of Ice Particles Formed by Release of $H_2O$ in Vacuum

THOMAS T. KASSAL*
*Grumman Aerospace Corporation, Bethpage, N.Y.*

## Introduction

LIQUID water droplets released in space during the Apollo missions quickly froze and formed luminous clouds of ice particles. The thermodynamics and optical properties of droplets formed in this manner have become a topic of current interest.[1,2] In the work reported herein, the scattering characteristics of an aggregate of ice particles formed by injecting a stream of water into a vacuum tank were determined experimentally. Although the experiments were performed in the absence of solar radiation, the laboratory freezing conditions are similar to those encountered during the Apollo flights. The measured optical properties are believed to be identical to those that would be observed from a cloud formed by release of a liquid from a spacecraft.

## Experimental

A concentrated flow of ice particles was formed by introducing a stream of water through a 0.4-mm orifice into an evacuated 325 $ft^3$ vacuum tank. The stream broke into individual particles while cooling. After they had frozen, the particles were collected and collimated by means of a 4-ft-mylar funnel placed approximately 10 ft from the water injection orifice. The funnel produces a vertical flow of frozen particles. The optical arrangement used for scattering measurements is shown in Fig. 1. Ice particles flow along the $z$ axis. A white light source produces a parallel beam that rotates in the $xy$ plane around the particle flow at a speed of approximately one rps. The scattered radiation is recorded by a stationary 1P21 photomultiplier tube located in the $xz$ plane and at an angle, $\phi$, with respect to the $z$ axis. The diameter of the ice flow was 2.5 cm, approximately twice as large as the light beam. High speed (4000 frames/sec) motion pictures were taken of the ice flow, and conventional photographs obtained at a shutter speed of 0.002 sec provided particle size distribution data. The absolute quantity of water evaporated during the cooling process was determined by attaching a calibrated glass tube, cooled by liquid nitrogen, to the base of the funnel. After collecting the ice particles in the tube, air was reintroduced into the vacuum tank and the ice particles were allowed to melt. By comparing the volume of water introduced into the tank with the collected volume, it was determined that approximately 80% of the water injected through 0.4- and 0.7-mm orifices evaporates during the cooling process. The experiments were repeated with a saturated solution of $CaCl_2$, but the droplets failed to freeze.

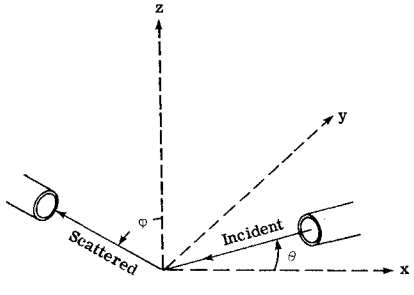


**Fig. 1 Optical arrangement for scattering experiments; ice particles flow along the $z$ axis.**

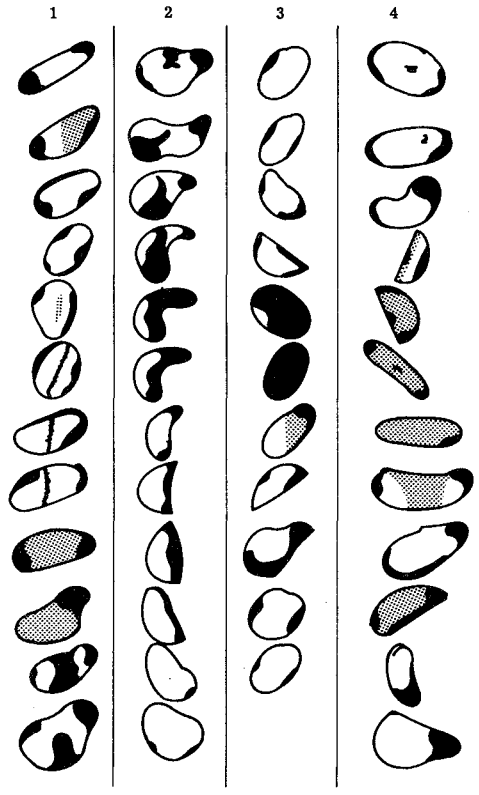


**Fig. 2 Reproductions of four particles tumbling during free fall; dark areas corespond to bright spots on the particles.**

## Results

The particle size distribution for a 0.4-mm orifice was obtained by measuring the size of each particle in a conventional photograph of the verticle flow. Particle size is defined here as the largest dimension of the particle.

**Table 1 Ice particle size distribution for a 0.4 mm orifice**

| Particle size, mm | 0–0.2 | 0.2–0.4 | 0.4–0.6 | 0.6–0.8 | 0.8–1.0 | 1.0–1.2 |
|---|---|---|---|---|---|---|
| Fraction of total particles | 0.27 | 0.26 | 0.21 | 0.17 | 0.07 | 0.02 |

High speed motion pictures of the flow, projected onto a large screen, made millimeter size particles appear to be 50 cm in

Received March 6, 1973; revision received August 28, 1973.
Index category: Atmospheric, Space and Oceanographic Sciences.
* Research Scientist.

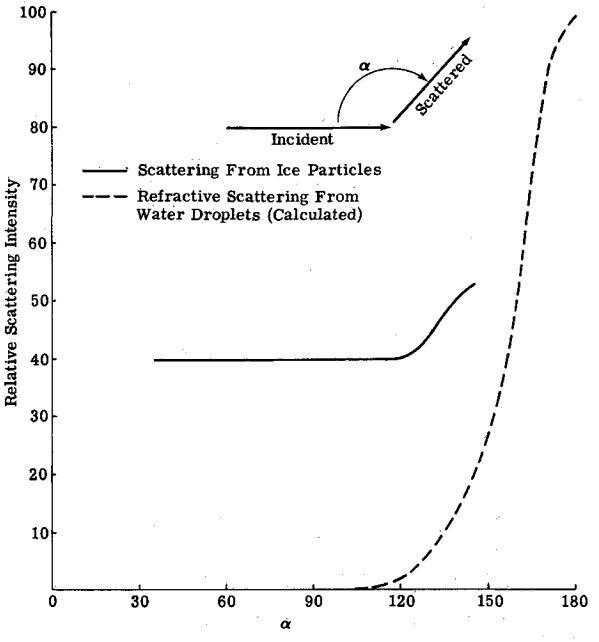


**Fig. 3 Measured scattering properties of an optically thin aggregate of ice particles compared to the calculated refraction pattern of a water droplet.**

diameter. By using a time and motion projector and copying successive frames, sketches of four particles were constructed (Fig. 2). Each column portrays one particle tumbling during free fall, illuminated by two floodlights located about 90° from the viewing direction. The dark areas in Fig. 2 correspond to bright spots on the particles, and white areas are nonscattering domains. It is difficult to ascertain three-dimensional shapes from the illustration, but it is evident from viewing the motion pictures that many particles are shaped like dishes and bowls.

The domains of intense scattering are determined by particle geometry (Fig. 2). It is not certain whether these bright areas are due to surface reflections or to refraction of transmitted light. It is certain that individual particles do not scatter isotropically and that their scattering patterns are not identical to the macroscopic pattern obtained from the aggregate of particles in these experiments.

The maximum value of $\phi$ with which the rotating system could be operated without recording direct radiation from the incident beam was 55°. In the absence of particles, no radiation is recorded at $\theta = 0°$. The particle density in the ice flow corresponds to an optically thin scattering cloud in the sense that approximately 75% of the incident radiation passes through the flow without encountering particles. The measured scattering characteristics of the ice particles are shown in Fig. 3. The scattering is symmetrical around the incident radiation axis, is constant for $\alpha$ between 35° and 120°, and then increases in the direction of the incident radiation. No data were obtained for $\alpha$ between 0°–35° or 145°–180° because of the limitation on $\phi$. The scattering pattern of polarized light leaving a water droplet surface after having undergone two refractions but no internal reflections, included in Fig. 3, was calculated from data in Ref. 3. A comparison of the two scattering patterns suggests that the intensity increase at 120° for ice particles is due to the refraction of transmitted light.

### A Physical Model

The scattering characteristics of an artificial ice cloud depend in part on the geometry of individual particles. A study of the high-speed motion pictures leads to the conjecture that many of the particles are fragments of larger droplets that broke apart during the freezing process. To prove the hypothesis, the thermodynamics of a cooling droplet was studied by assuming that the particle is spherical and that it consists of a series of $n$ concentric shells of radius $R(n)$ and temperature $T(n)$. The heat conducted through any shell from the interior of the droplet in time $t$ is given by

$$H = k[T(n+1) - T(n-1)]4\pi R^2(n)t/\Delta R$$

where $k$ is the thermal conductivity of water, $T(n+1)$ and $T(n-1)$ are the temperatures of the two adjacent shells, and $\Delta R$ is the shell thickness.

For a liquid in equilibrium with its vapor, the rate of collision of gaseous molecules with the liquid surface is given by $1/4\ Nu$ where $N$ and $u$ are the gaseous density and average velocity, respectively. Molecules leave the surface of the liquid at this same rate in a vacuum. The value of $N$ was calculated using the ideal gas law and the empirical vapor pressure of water as a function of temperature. The heat leaving the surface of a droplet is then given by

$$B\pi aNuR^2(n) \quad \text{(cal/sec)}$$

where $a$ is the accommodation coefficient and $B$ is the energy of vaporization of water, $1.7 \times 10^{-20}$ cal/molecule.

The dynamic situation of heat conduction from the interior shells to a surface cooled by evaporation was solved numerically. The results for a 2-mm particle consisting of 10 concentric shells are shown in Fig. 4 where the temperature of the four outer shells is plotted as a function of time. The curves terminate at the time required to freeze the outside shell, $6.2 \times 10^{-2}$ sec in this particular case. The temperature of the fourth shell remains constant at its initial value while the outer shell cools and freezes.

Since water expands as it freezes, the solid skin of a spherical water droplet experiences a large internal pressure increase as the thickness of the ice layer increases. The particle must ultimately crack before all the water freezes. The most plausible explanation for the bowl-shaped particles observed in these experiments is that a spherical particle breaks in half during the freezing process with a simultaneous loss of liquid from its interior. Ice particles resulting from this formation process could easily have all the observed various shapes.

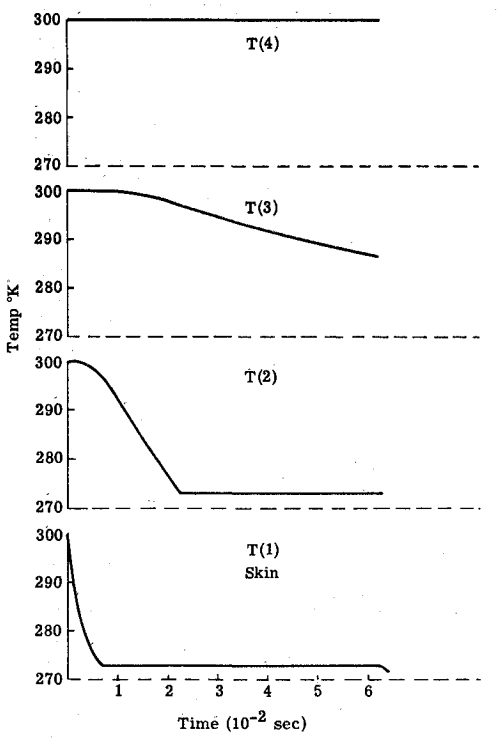


**Fig. 4 Temperature-time history of the outer four shells of a 2 mm droplet subdivided into 10 shells.**

### References

[1] Buffalano, C., "A Physical Model of the Apollo Oxygen Releases," *Journal of Geophysical Research*, Vol. 76, 1971, p. 27.

[2] Sharma, R. and Buffalano, C., "Temperature and Size Histories of Liquid $H_2$, $O_2$, and $H_2O$ Particles Released in Space," *Journal of Geophysical Research*, Vol. 76, 1971, p. 232.

[3] Van DeHulst, H., *Light Scattering by Small Particles*, Wiley, New York, 1957.


# Development of the Astrobee F Sounding Rocket System


R. B. JENKINS* AND J. P. TAYLOR†

*Aerojet Liquid Rocket Company, Sacramento, Calif.*

H. J. HONECKER JR.‡

*NASA Goddard Space Flight Center, Greenbelt, Md.*


### Introduction

THE Astrobee F sounding rocket vehicle was developed from a dual-thrust, long-burning, solid propellant rocket motor developed for the NASA Office of Aeronautics and Space Technology to demonstrate new propulsion technology. The concept for a dual-thrust extended burning solid rocket motor grew out of earlier studies performed for NASA-OAST. The first application of these concepts was the development of the 6-in. diameter dual-thrust Astrobee D which has previously been reported.[1] The Astrobee F propulsion system was an extension of the design concept utilizing hydroxyl-terminated polybutadiene (HTPB) propellant designed to have very low burning rates. A relatively neutral pressure history is maintained during the sustain portion of burning by use of a one piece molded plastic ablating nozzle.

An abbreviated static test program included four static firings augmented by a well-instrumented flight test which featured an attempt to recover the motor as well as the payload. Thus, the first flights of the vehicle became "high altitude static tests." Upon successful demonstration of the Astrobee F propulsion system, a vehicle design and flight test program was initiated by NASA Goddard Space Flight Center for the demonstration of the propulsion system as part of a complete sounding rocket vehicle (Fig. 1).

### Motor Development

The general concept of the Astrobee F was similar to that of the Astrobee D, in that the motor provides a dual-thrust level; a short, high-thrust level boost-phase followed by a relatively long, low-thrust level sustain phase. The extended sustain phase was to provide the advantages of a low level of drag, aerodynamic heating, and dynamic pressure, all of which have a significant effect on payload design and environment. The Astrobee F environment is similar to the liquid Aerobees.

There was concern that a one piece molded plastic nozzle similar to that used on the Astrobee D might not be scalable for use on a significantly larger size Astrobee F motor. Variations in molding technique, materials preparation and post cure were tried. These tests resulted in the largest known single piece molded nozzle. The nozzle, which is of a 13.5-in.-diam, uses 49 lb of glass phenolic material. The nozzle section thickness tapers from 3.5 in. to 0.5 in.

The first Astrobee F motor was fired on Dec. 2, 1970. The motor achieved the desired propulsion parameters and burned for a duration of 50 sec. Examination of the motor after firing, showed the internal insulation had eroded at a localized area in the aft section of the motor and that the case material had been heated to the point of distortion. Examination of the liner revealed that material remained through approximately 270° of the aft portion of the chamber, but that all material had been removed in a portion of one quadrant. A number of potential causes for this asymmetrical erosion were considered and what appeared to be a reasonable hypothesis was formulated.

The second unit was fired on Feb. 18, 1971. Propulsion-wise, it appeared to be nearly identical to FF01 with a smooth transition between the high-pressure boost and the low-pressure sustain portion, as predicted. Operation was normal through approximately 42 sec when the chamber pressure took a sharp drop. Upon examination, the motor was found to have burned through in one quadrant in the aft portion of the chamber. Subsequent examination of the linear system revealed an identical erosion pattern to that of FF01. That is, adequate insulation through three quadrants with one quadrant having been reduced to zero insulation. It became apparent from the results of this

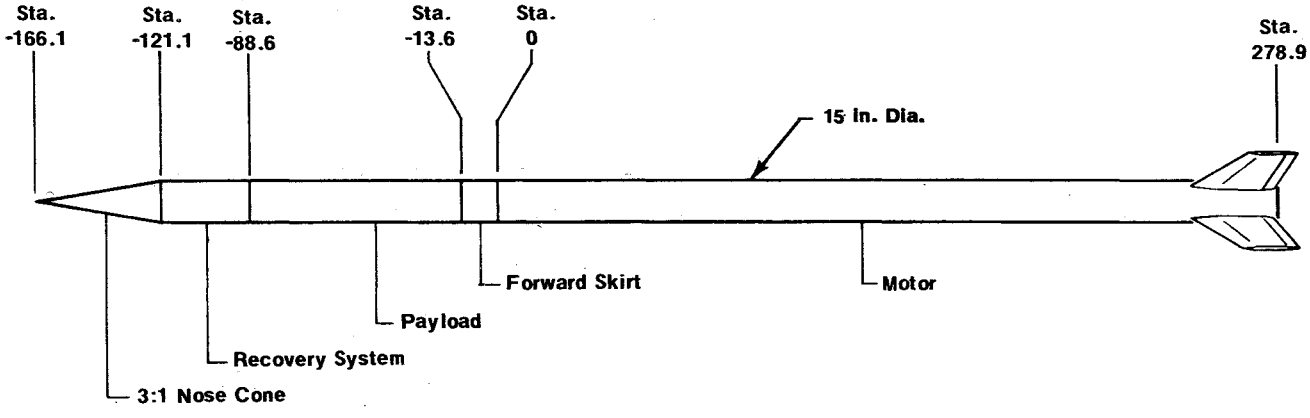


**Fig. 1 Astrobee F flight test vehicle.**


Presented as Paper 73-300 at the AIAA 3rd Sounding Rocket Technology Conference, Albuquerque, N.Mex., March 7-9, 1973; submitted April 13, 1973; revision received July 27, 1973.

Index categories: LV/M Propulsion System Integration; Sounding Rocket Systems; Solid and Hybrid Rocket Engines.


* Manager Astrobee Programs.

† Manager Engineering Analysis and Special Programs.

‡ Program Manager Performance Branch Sounding Rocket Division.